Proton inelastic scattering studies at the borders of the "island of inversion": The ^{30,31}Na and ^{33,34}Mg case

Z. Elekes,[1,2] Zs. Dombrádi,[1] A. Saito,[3] N. Aoi,[2] H. Baba,[3] K. Demichi,[3] Zs. Fülöp,[1] J. Gibelin,[4] T. Gomi,[3] H. Hasegawa,[3] N. Imai,[5] M. Ishihara,[2] H. Iwasaki,[5] S. Kanno,[3] S. Kawai,[3] T. Kishida,[2] T. Kubo,[2] K. Kurita,[3] Y. Matsuyama,[3] S. Michimasa,[5] T. Minemura,[2] T. Motobayashi,[2] M. Notani,[5] T. Ohnishi,[5] H. J. Ong,[5] S. Ota,[6] A. Ozawa,[7] H. K. Sakai,[3] H. Sakurai,[5] S. Shimoura,[5] E. Takeshita,[3] S. Takeuchi,[2] M. Tamaki,[5] Y. Togano,[3] K. Yamada,[3] Y. Yanagisawa,[2] and K. Yoneda[2]

[1]*Institute of Nuclear Research of the Hungarian Academy of Sciences, P.O. Box 51, Debrecen, H-4001, Hungary*

[2]*The Institute of Physical and Chemical Research, 2-1 Hirosawa, Wako, Saitama 351-0198, Japan*

[3]*Rikkyo University, 3-34-1 Nishi-Ikebukuro, Toshima, Tokyo 171-8501, Japan*

[4]*Institut de Physique Nucléaire, 15 rue Georges Clemenceau, F-91406 Orsay, France*

[5]*University of Tokyo, Tokyo 1130033, Japan*

[6]*Kyoto University, Kyoto 606-8501, Japan*

[7]*University of Tsukuba, Tennoudai 1-1-1, Tsukuba-shi, Ibaraki 305-8571, Japan*

(Received 5 December 2005; published 18 April 2006)

The paper reports on the ^{30,31}Na and ^{33,34}Mg proton inelastic scattering reactions studied at intermediate energy. The neutron and proton deformation of the four nuclei have been deduced and found to be strongly correlated by comparing the present (p, p') data with that of previous Coulomb excitation experiments. In the neutron-knockout channel a new state was found in ^{30}Na at 360 keV and the energies of the known γ-ray transitions have been confirmed in all the four nuclei.

DOI: 10.1103/PhysRevC.73.044314 PACS number(s): 21.60.Cs, 23.20.Lv, 25.40.Ep, 27.30.+t

I. INTRODUCTION

The phenomena associated with the breaking of the $N = 20$ shell closure far from stability are ascribed to the inversion of the (spherical) closed-shell configurations and the (deformed) multiparticle–multihole intruder configurations. This inversion appears in a rather limited area of the nuclear chart, the so-called "island of inversion", where nuclei gain correlation energy through particle–hole excitations across the $N = 20$ shell gap. The fact that several levels were observed at low excitation energy, e.g., in ^{31}Mg [1] or ^{29}Ne [2] is a clear indication for an influence of intruder states and suggests that the border of the "island of inversion" is close to $N = 19$. From theoretical point of view, there is a renewed interest in the placement of the border of the island since Monte Carlo shell model (MCSM) calculations [3] predict a significant reduction of the $d_{3/2}$–$f_{7/2}$, $p_{3/2}$ neutron shell gap at ^{28}O to 1.2 MeV, which can be compared to the large 5 MeV value of the *sd* shell model, e.g, in Ref. [4]. Consequently, MCSM calculations widen the "island of inversion" to lighter elements. The low energy of the 2_1^+ state in the $N = 18$ nuclei of ^{30}Mg [5] and especially ^{28}Ne [6] may also be considered as a signature of a structural change, which may arise as a consequence of mixing of normal and intruder configurations [3]. Recent observations of core-coupled states in ^{29}Na [7] and ^{27}F [8] confirm the tendency of lowering of 2^+ core states with decreasing atomic number. The detection of an intruder 0_2^+ state in ^{28}Ne [9] and an intruder state in ^{27}Ne [10] may pose a limit on the size of the $N = 20$ shell gap [10]. In order to contribute to the mapping of the borders of the "island of inversion", (p, p') investigations were carried out to study the energy level structure of ^{30,31}Na and ^{33,34}Mg nuclei. This process was also suitable to deduce the deformation of these isotopes and check the neutron decoupling phenomenon [11–13] in this region by comparing the proton and neutron distributions.

II. EXPERIMENTAL

The experiment was performed at the RIKEN Accelerator Research Facility. The schematic view of the experimental setup can be seen in Fig. 1. A ^{40}Ar primary beam of 94 MeV/nucleon energy with 60 pnA intensity was transported to a ^{181}Ta production target of 0.5 mm thickness. The RIPS [14] fragment separator analyzed the momentum and mass of the reaction products. The ^{30,31}Na and ^{33,34}Mg beams were produced in two individual runs with different settings of Bρ values. An aluminum wedged degrader of 221 mg/cm^2 was put at the momentum dispersive focal plane (F1) for purifying the constituents. In the first run of ^{30,31}Na, the secondary beam included neutron-rich O, F, Ne and Na nuclei with $A/Z \approx 3$ while mainly Mg and Al isotopes were mixed in the second run of ^{33,34}Mg. The fragment separator was set to its full 6% momentum acceptance to achieve as high beam intensities as possible. The total intensity was about 100 particle/s (pps) for both runs, while the ^{30,31}Na/^{33,34}Mg intensities reached 8, 6, 3 and 2 pps, respectively, on average. The identification of incident beam species was performed on an event-by-event basis by means of energy loss, time-of-flight (TOF) and magnetic rigidity ($B\rho$) [15]. Determining the $B\rho$ values by a parallel plate avalanche counter (PPAC), the position of the fragments at F1 was also measured. The sensitive area of this PPAC was 15 × 10 cm^2 which covered the total momentum range of the secondary beam. Two plastic scintillators of 1 mm thicknesses were placed at the first and second focal planes (F2 and F3) to measure the TOF. One silicon detector with thickness of 0.35 mm was inserted at F3 for energy loss

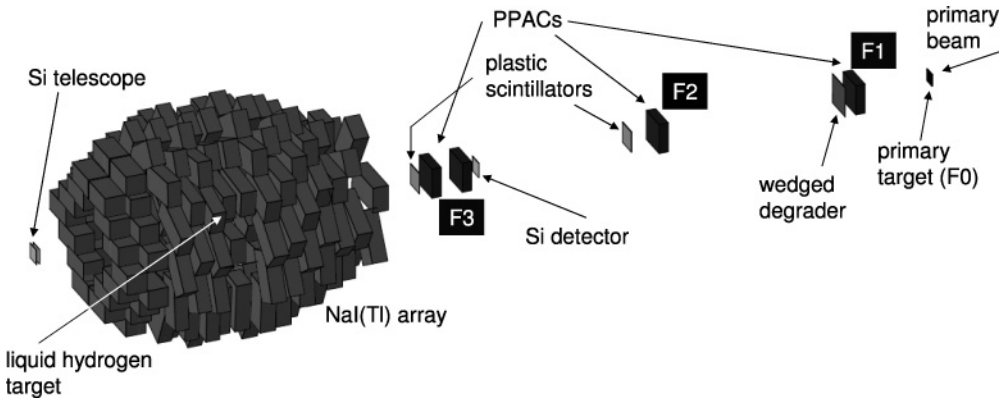

FIG. 1. Layout of the experimental setup.

determination. The separation of the isotopes was complete, which is demonstrated in Fig. 2 for the Na run.

The secondary beam hit a liquid hydrogen target [16] of 30 mm diameter the thickness of which was 24 mm and its entrance and exit windows were made of 6.6 μm Aramid foil. The average areal density of the hydrogen cooled down to 22 K was 210 mg/cm^2. The mean energy of the isotopes in the target was around 50 MeV/nucleon. Two PPACs at F3 upstream of the target monitored the position of the incident particles. The beam spot size was 24 mm both in horizontal and vertical directions. The reaction products and scattered particles were detected and identified by a PPAC and a silicon telescope of three layers with thicknesses of 0.5, 0.5 and 1 mm located about 80 cm downstream of the target. Each layer was made of a 2 × 2 matrix of detectors the active area of which was 48 × 48 mm^2. The Z identification was performed by TOF-energy loss method where the TOF was taken between the PPACs upstream and downstream of the secondary target. The isotope separation was done by use of the ΔE–E method. The mass spectra are dominated by the beam particles, however requiring coincidence with γ rays, we could eliminate the non-interacting or elastically scattered part of the beam making the ΔE–E method sensitive enough. It is demonstrated in Fig. 3 where the linearized mass spectrum of sodium isotopes is shown for the 2 × 2 matrix Si-telescope (events from ^{30}Na and ^{31}Na beams are added). The ΔE–E curves in each detector were linearized by second degree polynomial functions. In case of Mg isotopes, similar separation could be achieved.

The separation of the isotopes can be further checked with the scatter plot of mass number vs. γ ray energy, which is seen in Fig. 4. Although the statistics is low, the γ rays corresponding to the different Na nuclei are distinct.

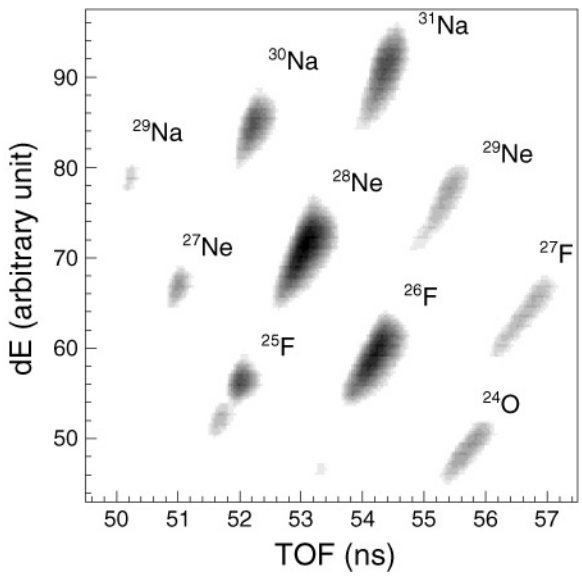

FIG. 2. Isotope separation of the incoming "cocktail" beam for the Na run.

III. RESULTS AND DISCUSSION

The deexciting γ rays emitted by the inelastically scattered nuclei were detected by the DALI2 setup consisting of

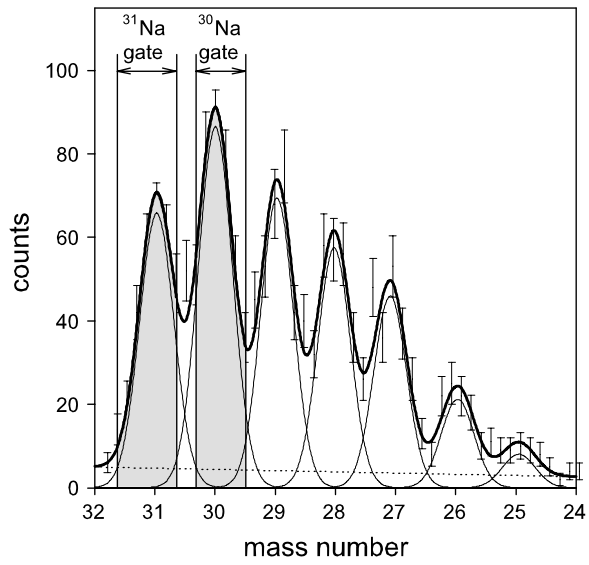

FIG. 3. Separation of sodium isotopes using ΔE–E information in the silicon telescope produced in coincidence with γ-rays. The bold solid line is a sum of seven Gaussian functions and a polynomial background. The individual Gaussians and the background function are also plotted with thin solid and dotted lines, respectively.

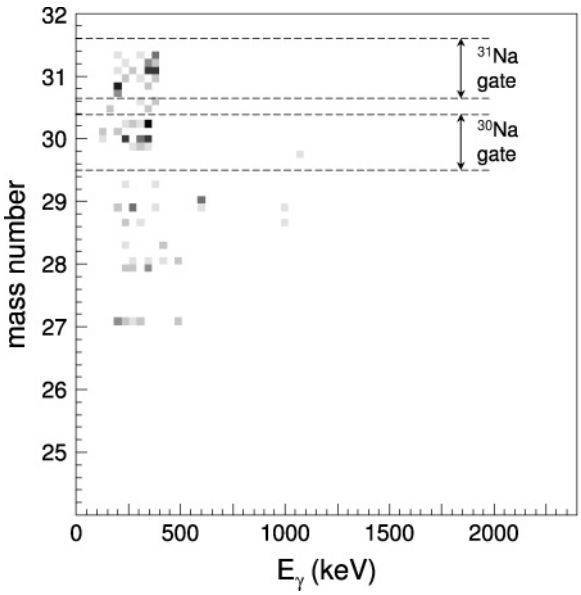

FIG. 4. Mass number of Na isotopes plotted against the γ ray energy.

146 NaI(Tl) scintillators [17] surrounding the target. The energy calibration of the detectors was made by standard ^{22}Na, ^{60}Co, and ^{137}Cs radioactive sources. The intrinsic energy resolution of the array was 10% (FWHM) for a 662 keV energy γ ray. In Fig. 5 the Doppler-corrected γ ray spectra for ^{1}H(^{31}Na,^{31}Na) (a), ^{1}H(^{31}Na,^{30}Na) (b), and ^{1}H(^{30}Na,^{30}Na) (c) reactions are presented, which were produced putting an additional gate on the time spectra of the NaI(Tl) detectors selecting the prompt events. Figure 6 shows similar spectra for ^{1}H(^{34}Mg,^{34}Mg) (a), ^{1}H(^{34}Mg,^{33}Mg) (b), and ^{1}H(^{33}Mg,^{33}Mg) (c) reactions.

By fitting the spectra with Gaussian functions and smooth exponential backgrounds, first, the positions of the peaks were determined to be 370(12) keV (a), 360(13) keV (b), and 403(18) keV (c) for Na nuclei. Although the energies in panel (a) and (b) are quite close to each other, the line in panel (b) can clearly be associated to ^{30}Na. The possible leakthrough from ^{31}Na is less than 5% based on the mass spectrum in Fig. 3. Similarly, in the spectra of Mg isotopes, peaks at 685(16) keV (a), 484(20) keV, 561(17) keV (b), and 483(17) keV (c) were observed. During the fitting process, the widths of the peaks were fixed to the expected values including the intrinsic resolution and Doppler effect. The quoted uncertainties of the peak positions are the square roots of the sum of the squared uncertainties including two main errors, namely, the statistical one and the one due to the uncertainty of the Doppler correction.

For ^{31}Na, a 350(20) keV peak was previously observed in a reaction on ^{197}Au target [18] which coincides with our value of 370(12) keV. For ^{30}Na, only a single peak was detected earlier [19] at 433(16) keV. It slightly differs from our value of 403(18) keV, however they overlap within 1σ limit. It is worth mentioning that the peak positions for ^{30}Na in panel (b) and (c) of Fig. 5 are different, the peak observed in the neutron removal channel is at 360(13) keV.

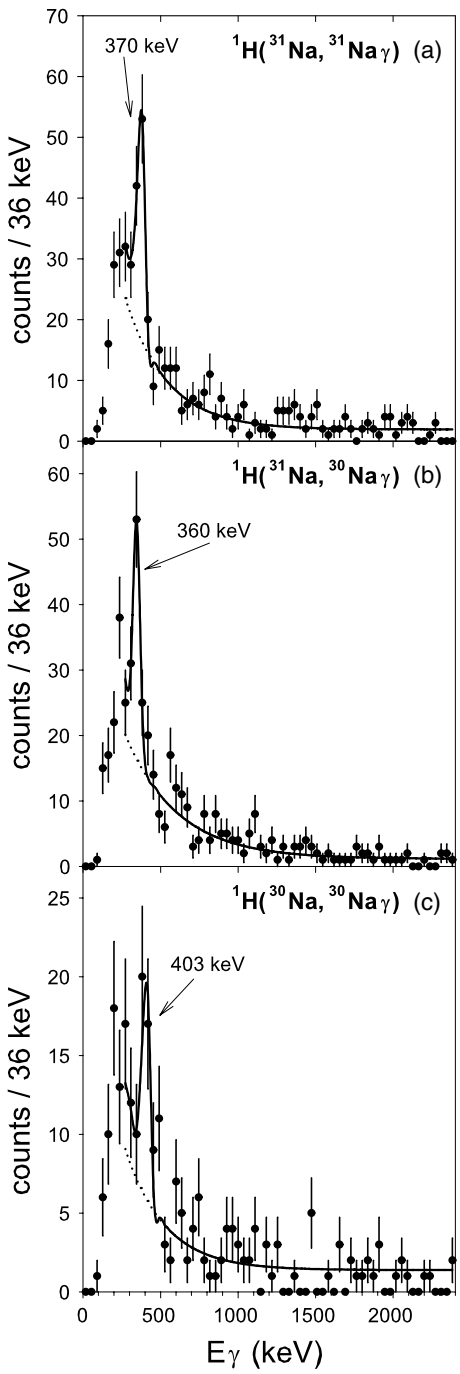

FIG. 5. Doppler-corrected spectra of γ rays emerging from ^{1}H(^{31}Na,^{31}Na) (a), ^{1}H(^{31}Na,^{30}Na) (b), and ^{1}H(^{30}Na,^{30}Na) (c) reactions. The solid line is the final fit including the spectrum curves from GEANT4 simulation and additional smooth polynomial backgrounds plotted as separate dotted lines for each nucleus.

The energy for the first excited state of ^{34}Mg was previously determined to be 660(10) [20] and 656(7) keV [21] which overlap with the present value [685(16) keV] within 1σ limit. For ^{33}Mg, several peaks were detected in a β decay study earlier [22] including 484.1(1) keV and 546.2(1) keV ones matching our two lines at 484(20) keV and 561(17) keV shown in Fig. 6(b). In a Coulomb excitation measurement,

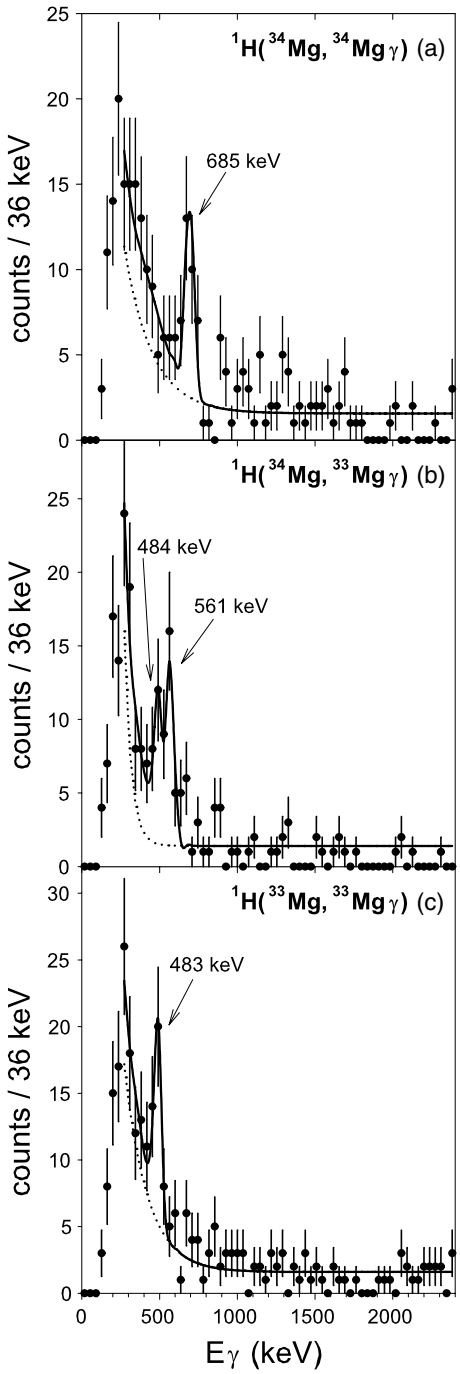

FIG. 6. Doppler-corrected spectra of γ rays emerging from ^{1}H(^{34}Mg,^{34}Mg) (a), ^{1}H(^{34}Mg,^{33}Mg) (b), and ^{1}H(^{33}Mg,^{33}Mg) (c) reactions. The solid line is the final fit including the spectrum curves from GEANT4 simulation and additional smooth polynomial backgrounds plotted as separate dotted lines for each nucleus.

a single peak at 485(1) keV also appeared in the ^{33}Mg spectrum [23]. A 490 keV line was also observed in the double step fragmentation process [20].

The neutron knockout reaction can excite even such states which are weakly connected to the ground state. Since low-lying intruder states are expected in all the nuclei investigated, observation of γ rays not seen in the inelastic scattering process may be a sign of excitation of intruder states with parities opposite to the parity of the ground state. Indeed, in ^{33}Mg, the 546 keV and 484 keV peaks were assigned to the decay of different parity states from a β decay study [22], and it was shown in the Coulomb excitation experiment [23] that it is the 484 keV state which has the same parity as the ground state. Our results support these findings. For ^{30}Na, the 403 keV line is strongly excited in the inelastic scattering and the same sign of the parity of the ground state can be assigned to it. The 360 keV line, not seen in the Coulomb excitation [19], may arise from the decay of a state with different parity, but in this case it seems to be quite unlikely that the state associated to the 403 keV peak populated in the inelastic scattering is not excited in the neutron removal process. Because of the limited resolution of our setup, the 360 keV and the 403 keV lines can easily overlap. Therefore, we investigated the possibility that the peak in panel (b) of Fig. 5 is a doublet assuming a second line at an average value of 417(12) keV (from 403(18) keV and 433(16) keV [19]). We found that up to 12% of the intensity of the 360 keV peak may arise from the higher energy γ ray. Similarly, the possibility of having some 360 keV component in the 403 keV line cannot be excluded. Even though, the situation is rather different from ^{33}Mg. The negligible excitation of the state observed in the (p, p') channel by neutron removal process may indicate that the difference between the two ways of excitations is not in the neutron but the proton configurations. We raise the possibility, which calls for theoretical calculations, that the proton configuration of the ground state of ^{30}Na nucleus differs from that of ^{31}Na. Thus, the removal of a neutron from ^{31}Na can lead to states disjunct with the ^{30}Na ground state configuration, even if the neutron configurations are similar. Since the ^{31}Na ground state is known to be of $\pi[d^3_{5/2}]_{3/2}$ nature, it seems to be reasonable to assume that the ^{30}Na has the natural $\pi[d^3_{5/2}]_{5/2}$ proton configuration in its ground state.

To determine the cross sections of the production of the γ rays in proton inelastic scattering the peak positions determined were fed into the detector simulation software GEANT4 [24] and the resultant response curves plus smooth polynomial backgrounds were used to analyze the experimental spectra. The simulations were able to reproduce the efficiencies measured for static calibration sources to an accuracy of 8% (included in the error calculations) and were then applied to take into account the velocities and focussing of the particles according to the experimental parameters. The observed cross sections are listed in Table I.

From a distorted wave analysis of the cross sections, we derived "matter" deformation parameters (β_M). In the calculations, the standard collective form factors were applied and the global phenomenological parameter set CH89 proposed in Ref. [25] was employed for the optical potential. We assumed a $\Delta J = 2$ transition for ^{34}Mg and $\Delta J = 1$ transitions for ^{33}Mg and ^{30,31}Na nuclei. The determined values only slightly depend on the assumption of different initial and final spin values. The "matter" deformation parameters deduced in this way can be found in Table I. The mass deformations of these nuclei are consistent with their charge deformations determined from Coulomb excitation experiments, which can be also seen

TABLE I. Angle integrated cross sections of the (p, p') process corrected for the detection efficiency and deformations for ^{30,31}Na and ^{33,34}Mg nuclei.

Isotope (peak)	Cross section	β_M	β_C	β_n
^{31}Na (370 keV)	24 ± 4 mb	0.56 ± 0.05 ($5/2^+_1 \rightarrow 3/2^+_{\text{g.s.}}$)	0.66 ± 0.16 [19]	0.54 ± 0.07
^{30}Na (403 keV)	18 ± 4 mb	0.32 ± 0.04 ($3^+_1 \rightarrow 2^+_{\text{g.s.}}$)	0.41 ± 0.10 [19]	0.30 ± 0.05
^{34}Mg (685 keV)	111 ± 37 mb	0.68 ± 0.16 ($2^+_1 \rightarrow 0^+_{\text{g.s.}}$)	0.58 ± 0.06 [21]	0.70 ± 0.13
^{33}Mg (483 keV)	33 ± 10 mb	0.47 ± 0.08 ($7/2^+_1 \rightarrow 5/2^+_{\text{g.s.}}$)	0.52 ± 0.12 [23]	0.46 ± 0.10

in Table I. As we discussed in Ref. [13], there might be an additional error on the retrieved deformation parameters because of the choice of the optical potential and the size of this error is around 10–20%.

Based on the "matter" and charge deformation parameters and using the formula of

$$(Nb_n + Zb_p)\,\delta_M = Nb_n\delta_n + Zb_p\delta_p, \qquad (1)$$

the neutron deformation parameters (see Table I) could also be extracted where $\delta_{n,p} = \beta_{n,p}R$ (assuming $\delta_p = \delta_C$) and R, N and Z are the nuclear radius, the neutron and the proton numbers, respectively, while $b_n/b_p = 3$ are the sensitivity parameters for protons and neutrons of our (p, p') probe.

The results show that all these nuclei are largely deformed; the deformation of the proton and neutron distributions are similar and cannot be distinguished at the present experimental uncertainties. It is also noted that for ^{30}Na we assumed a single peak to be present at 403(18) keV in the (p, p') channel and identical to the one detected by Pritychenko *et al.* [19].

IV. CONCLUSIONS

Summarizing our results, we have studied the structure of ^{30,31}Na and ^{33,34}Mg nuclei by proton inelastic scattering. ^{30}Na and ^{33}Mg were also excited via neutron-knockout reaction in different ways. In ^{33}Mg, the neutron-knockout channel partly overlapped with the inelastic scattering channel, while for ^{30}Na it took a completely different excitation path. This difference can be assigned to a possible difference of proton configurations of the ground states of the target and the final nuclei. From the cross section of the inelastic scattering process the mass deformations were deduced for all the four isotopes, and from a comparison with the results of the Coulomb excitation experiments, the neutron deformations were also derived. All the investigated nuclei have significant mass deformation in agreement with the conclusions of the Coulomb excitation studies, and the neutron deformations do not differ from those of the charge deformations within experimental error, showing that the proton and neutron deformations are in phase as it is expected for usual deformed nuclei.

ACKNOWLEDGMENTS

We would like to thank the RIKEN Ring Cyclotron staff for their assist during the experiment. One of authors (Z.E.) is grateful for the JSPS Fellowship Program in RIKEN and thanks the support from OTKA F60348. The European authors thank the kind hospitality and support from RIKEN. The present work was partly supported by the Grant-in-Aid for Scientific Research (No. 1520417) by the Ministry of Education, Culture, Sports, Science and Technology and by OTKA T38404, T42733 and T46901.

[1] H. Scheit *et al.*, Nucl. Phys. **A746**, 96c (2004).
[2] Y. Yanagisawa *et al.*, Phys. Lett. **B566**, 84 (2003).
[3] Y. Utsuno, T. Otsuka, T. Mizusaki, and M. Honma, Phys. Rev. C **60**, 054315 (1999).
[4] E. Warburton, J. A. Becker, and B. A. Brown, Phys. Rev. C **41**, 1147 (1990).
[5] C. Detraz, D. Guillemaud, G. Huber, R. Klapisch, M. Langevin, F. Naulin, C. Thibault, L. C. Carraz, and F. Touchard, Phys. Rev. C **19**, 164 (1979).
[6] F. Azaiez *et al.*, AIP Conf. Proc. **495**, 171 (1999).
[7] V. Tripathi *et al.*, Phys. Rev. Lett. **94**, 162501 (2005).
[8] Z. Elekes *et al.*, Phys. Lett. **B599**, 17 (2004).
[9] M. Belleguic *et al.*, Phys. Rev. C **72**, 054316 (2005).
[10] Zs. Dombradi *et al.*, Phys. Rev. Lett., accepted, in press.
[11] Z. Elekes *et al.*, Phys. Lett. **B586**, 34 (2004).
[12] N. Imai *et al.*, Phys. Rev. Lett. **92**, 062501 (2004).
[13] Z. Dombrádi *et al.*, Phys. Lett. **B621**, 81 (2005).
[14] T. Kubo *et al.*, Nucl. Instrum. Methods B **70**, 309 (1992).
[15] H. Sakurai *et al.*, Phys. Lett. **B448**, 180 (1999).
[16] H. Ryuto *et al.*, Nucl. Instrum. Methods A **555**, 1 (2005).
[17] S. Takeuchi *et al.*, RIKEN Accel. Prog. Rep. **36**, 148 (2003).
[18] B. V. Pritychenko, T. Glasmacher, B. A. Brown, P. D. Cottle, R. W. Ibbotson, K. W. Kemper, L. A. Riley, and H. Scheit, Phys. Rev. C **63**, 011305(R) (2000).
[19] B. V. Pritychenko, T. Glasmacher, P. D. Cottle, R. W. Ibbotson, K. W. Kemper, K. L. Miller, L. A. Riley, and H. Scheit, Phys. Rev. C **66**, 024325 (2002).
[20] K. Yoneda *et al.*, Phys. Lett. **B499**, 233 (2001).
[21] H. Iwasaki *et al.*, Phys. Lett. **B522**, 227 (2001).
[22] S. Nummela *et al.*, Phys. Rev. C **64**, 054313 (2001).
[23] B. V. Pritychenko, T. Glasmacher, P. D. Cottle, R. W. Ibbotson, K. W. Kemper, L. A. Riley, A. Sakharuk, H. Scheit, M. Steiner, and V. Zelevinsky, Phys. Rev. C **65**, 061304(R) (2002).
[24] S. Agostinelli *et al.*, Nucl. Instrum. Methods A **506**, 250 (2003).
[25] R. Varner *et al.*, Phys. Rep. **201**, 57 (1991).